NOTES AND CORRESPONDENCE

The Role of GOES Satellite Imagery in Tracking Low-Level Moisture

DAN BIKOS, JOHN F. WEAVER,* AND JEFF BRAUN

Cooperative Institute for Research in the Atmosphere, Colorado State University, Fort Collins, Colorado

(Manuscript received 8 April 2005, in final form 19 September 2005)

ABSTRACT

This note provides examples of how geostationary satellite data can be applied to augment other data sources in tracking warm, moist air masses as they move northward from the Gulf of Mexico. These so-called returning air masses are often a key ingredient in bringing about severe weather outbreaks in the central and southeastern United States. The newer NOAA–GOES imagery provides high spatial and temporal resolution. Together, surface observations, upper-air soundings, and high-resolution satellite imagery provide a comprehensive picture of the returning moist air mass.

1. Introduction

The fact that low-level moisture is an important ingredient in the development of severe thunderstorms has been well documented over the previous century (Humphreys 1926; Showalter and Fulks 1943; Fawbush et al. 1951; Appleby 1954; Whitney and Miller 1956; Miller 1972; Schaefer 1986). It has also been shown that the Gulf of Mexico is the primary source of this low-level moisture in the United States east of the Rocky Mountains (Newton 1963). There have been a number of studies focusing on the return of low-level moisture from the Gulf of Mexico (Johnson 1976; Karnavas 1978; Henry 1979a,b; Lewis et al. 1989; Lewis and Crisp 1992; Crisp and Lewis 1992). Low-level moisture can be "cut off" when cold fronts—with their attendant northerly winds, cooler temperatures and low humidity—sweep in from the north. This incursion of cooler, drier air into the Gulf of Mexico occurs most frequently in the winter months with a gradual decrease through the spring months (Henry 1979a).

For the severe weather forecaster, an important component of the forecast problem is anticipating when warm, moisture-laden gulf air will advect northward, and in what quality or magnitude it will arrive. Weiss (1992) concludes that one of the chief errors in modeling moisture return is the lack of sufficient surface observations over the Gulf of Mexico (i.e., poor initialization). Although models have improved since this study, and the number of maritime observations has increased, the evaluation of the rapidly evolving severe storm environment rests on the subjective judgement of the forecaster. The process generally begins with the analysis of surface observations followed by the analysis of upper-air observations to quantify the depth and character of the returning air mass. However, the density of upper-air observations is still insufficient in giving us a complete picture (Schwartz and Doswell 1991). Total precipitable water (TPW) derived from satellite data and from upper-air observations has also been shown to be useful in analyzing gulf moisture returns (Rabin et al. 1991, 1992, 1993). However, the TPW products derived from the Geostationary Operational Environmental Satellite (GOES) are not possible whenever a relatively solid middle- or upper-level cloud deck is present. Other ground-based remote sensing

* Additional affiliation: NOAA/NESDIS/RAMM Team, Fort Collins, Colorado.

Corresponding author address: Dan Bikos, Cooperative Institute for Research in the Atmosphere, Regional and Mesoscale Meteorology Team, Colorado State University, W. Laporte Avenue, Fort Collins, CO 80523-1375.
E-mail: bikos@cira.colostate.edu

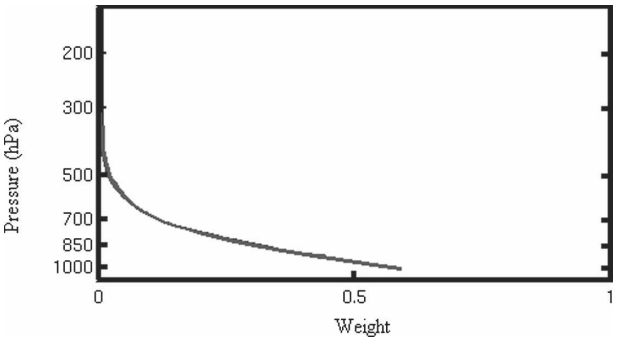

FIG. 1. Response curve for the weighting function of the 10.7-μm imaging channel on *GOES-12* (valid for the midlatitude standard atmosphere).

techniques such as the slant global positioning system (Bevis et al. 1992) and the atmospheric emitted radiance interferometer (Feltz et al. 1998) have also been used to gauge water vapor content in the lower atmosphere.

The purpose of this note is to illustrate the role of geostationary satellite imagery in tracking low-level moisture during the day or night. The surface observations provide approximate position (when used as an overlay with satellite imagery) and some quantitative information about the returning moist air mass. Upper-air soundings give a coarse representation of the magnitude and depth of the moisture. Utilizing a blend of satellite imagery, upper-air soundings, and surface observations provides the most complete diagnosis of the returning moist air mass. The analysis techniques used in this paper will focus on the role of the GOES imager in tracking low-level moisture, specifically, defining more precisely the boundaries between dry and moist air masses. These analysis techniques have been available for some time (e.g., Parmenter 1976), however, the study did not elaborate on differences due to time of day and/or cloud cover. Parmenter's study was also accomplished using the coarser-resolution satellite imagery available 30 years ago on the so-called Synchronous Meteorological Satellite series. The newer GOES imagery provides much improved spatial and temporal resolution (Menzel and Purdom 1994). GOES data frequently allow the forecaster to follow the progression of returning moisture through satellite loops where the speed of the moisture front can be obtained and its interaction with the mesoscale environment can be observed and evaluated. Advantages to this methodology include a more precise location of the moisture front, especially where observations are coarse. Disadvantages include mid- and upper-level clouds obscuring the lower levels.

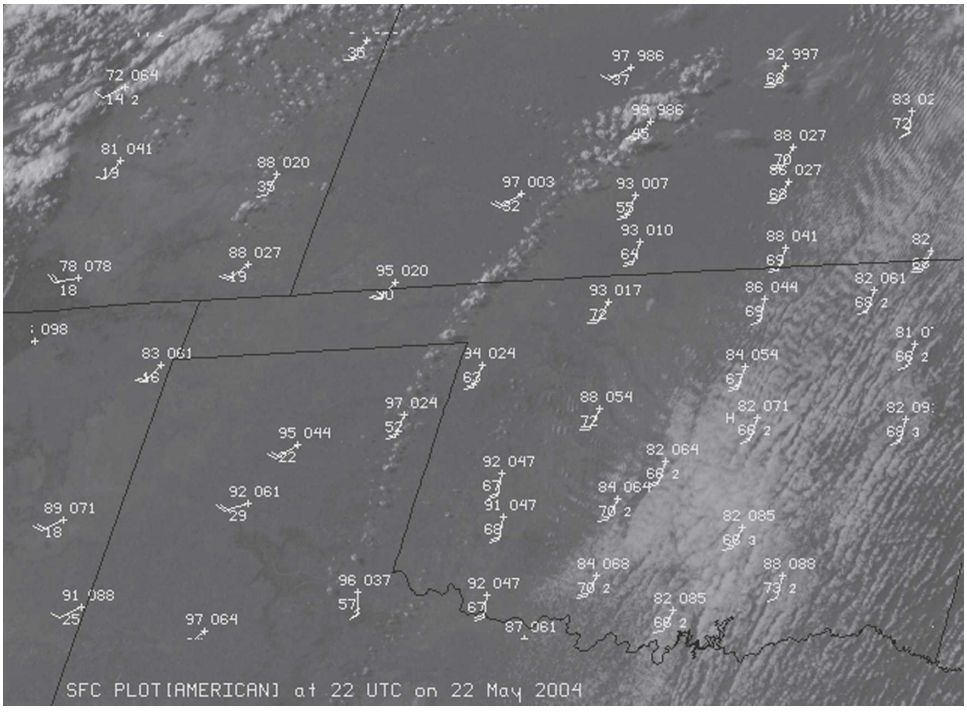

FIG. 2. *GOES-12* visible image from 2215 UTC 22 May 2004 with surface observations overlaid. Station plots are U.S. convention.

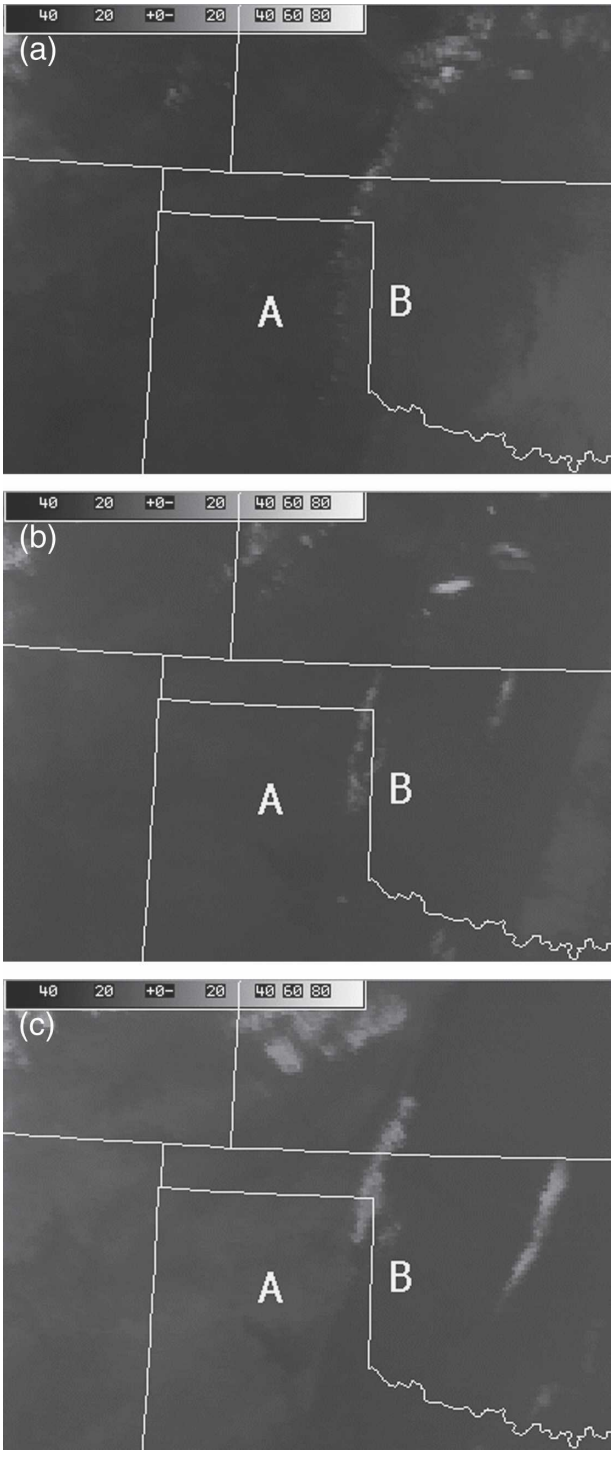

FIG. 3. *GOES-12* 10.7-μm images from (a) 2215 UTC 22 May 2004, (b) 0055 UTC 23 May 2004, and (c) 0245 UTC 23 May 2004. In the color table, warmer (cooler) brightness temperatures are darker (lighter). Points A and B represent the location of the dry and moist side of the dryline, respectively.

2. Examples of returning moisture in clear skies

During both the day and night, GOES infrared imagery can often be useful in detecting low-level warm-sector air masses (Parmenter 1976). If skies are clear, there must be sufficient thermal contrast between the encroaching air mass and that which it is replacing if detection is to be possible using the infrared alone. The thermal contrast over land is observed because of the more rapid rate of warming (cooling) in dry air during the day (night) as opposed to that of moist air. Just how much thermal contrast in the 10.7-μm channel is sufficient, will be addressed in example one (below). The capability to detect this contrast is possible because of the nature of the weighting function for the 10.7-μm channel. Figure 1 illustrates the response curve of the weighting function for the 10.7-μm channel in a standard atmosphere. The majority of the response comes from the surface through the near-ground region of the atmosphere.

Example 1: Use of infrared imagery during the day versus night (clear skies)

During daylight hours, the infrared imagery depicts a moist air mass as cooler. The visible imagery in Fig. 2 shows a line of clouds extending from the eastern Texas Panhandle northward into Kansas with clear skies on either side; the surface observations indicate this is a dryline. Infrared imagery in Fig. 3 shows the change in appearance of the moist and dry air masses as differential heating (cooling) occurs in the late afternoon (Fig. 3a), near sunset (Fig. 3b), and after sunset (Fig. 3c). Figure 4 shows the magnitude of the 10.7-μm brightness temperature difference between points A and B (shown in Fig. 3) versus time. During the daytime (nighttime), the dry air mass (point A) heats (cools) faster than the moist air mass (point B). Around both sunset and sunrise, the magnitude of the thermal contrast decreases across the moist–dry boundary so that it is no longer discernible (Fig. 3b). In the plot shown (Fig. 4), when the thermal contrast goes below about 3°C the boundary between the moist and dry air becomes indeterminate. Therefore, the tracking of the low-level moisture boundary is nearly continuous except for those periods of time that lack sufficient thermal contrast. The length of these periods will depend upon the magnitude of the difference in brightness temperature. Over large bodies of water, there is little or no thermal contrast, therefore the moisture boundary is indeterminate.

During nighttime hours, however, a moist air mass will show up as warmer in the infrared imagery. Figure 5 shows that the air mass in western Texas and New

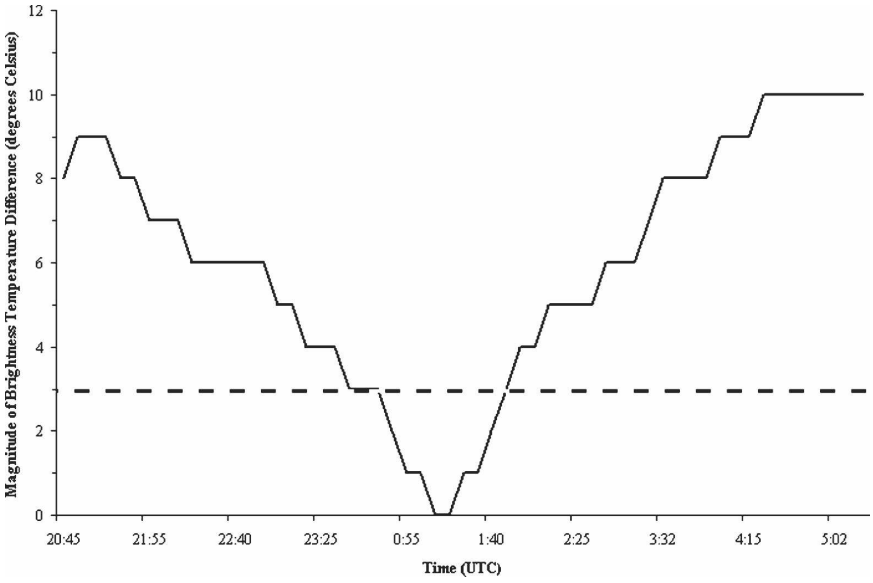

FIG. 4. Plot of the magnitude of the brightness temperature difference (solid line) between points A and B (shown in Fig. 3) vs time. The dashed line corresponds to a 3°C brightness temperature difference. Below this value, the boundary between the moist and dry air becomes indeterminate on the imagery.

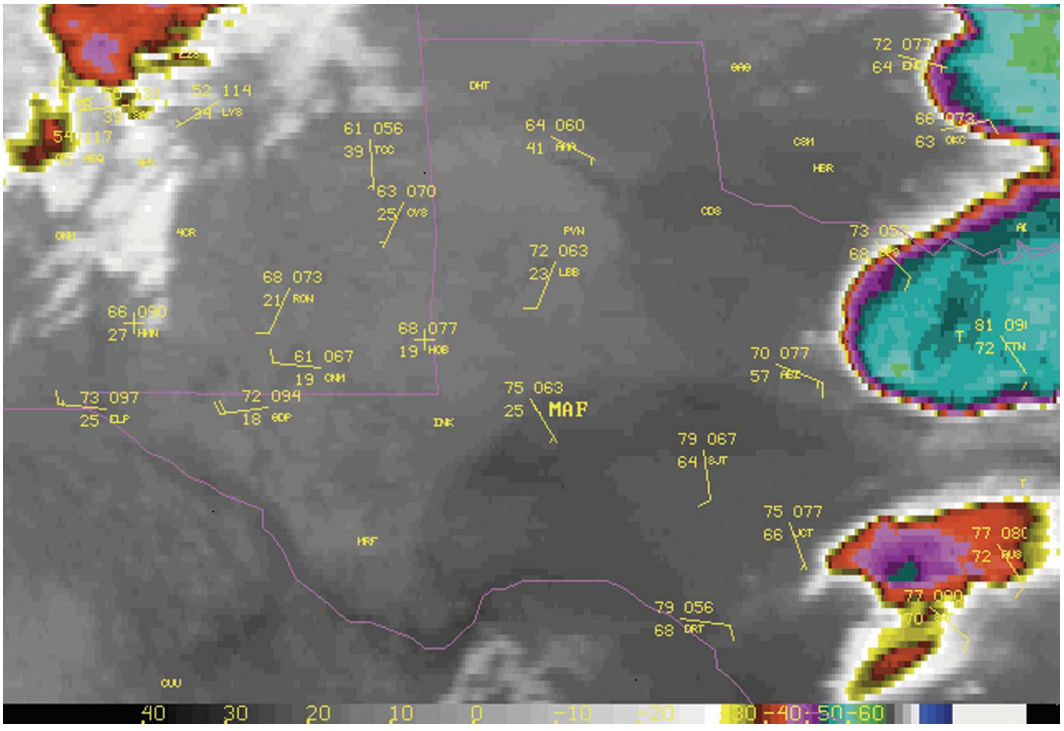

FIG. 5. *GOES-6* 11.2-μm image from 0349 UTC 13 May 1985, with surface observations overlaid. Station plots are U.S. convention. Note the wavelength of the longwave infrared channel is 11.2 μm rather than 10.7 μm as in the current GOES instrument.

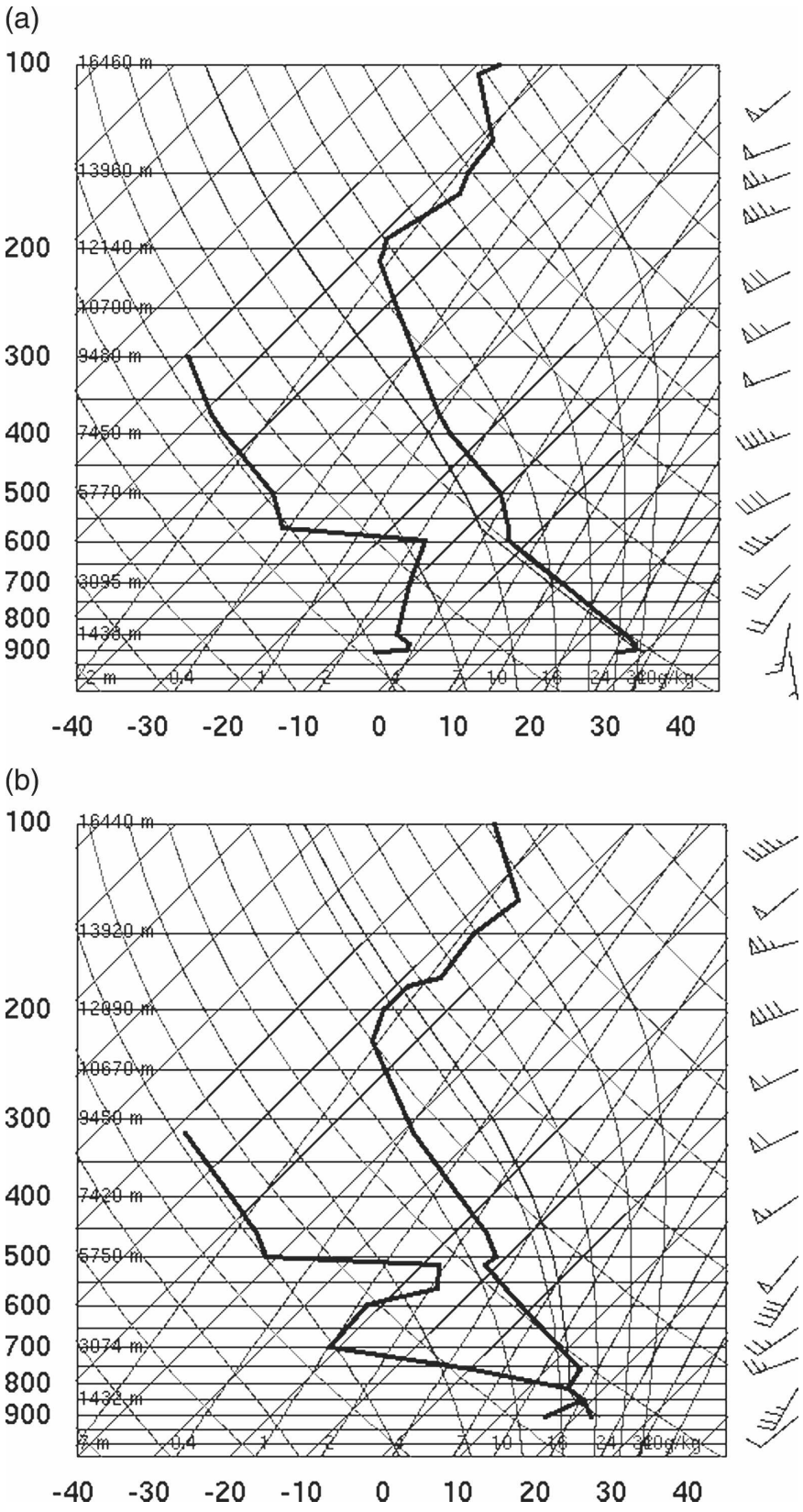

FIG. 6. Sounding for Midland, TX (MAF in Fig. 5) at (a) 0600 UTC 13 May 1985 (dry air mass just before the moisture advected into Midland) and (b) 1200 UTC 13 May 1985 [moisture (darker region in Fig. 5) advected into Midland by this time]. Wind speeds are in knots (1 kt = 0.5144 m s^{-1}).

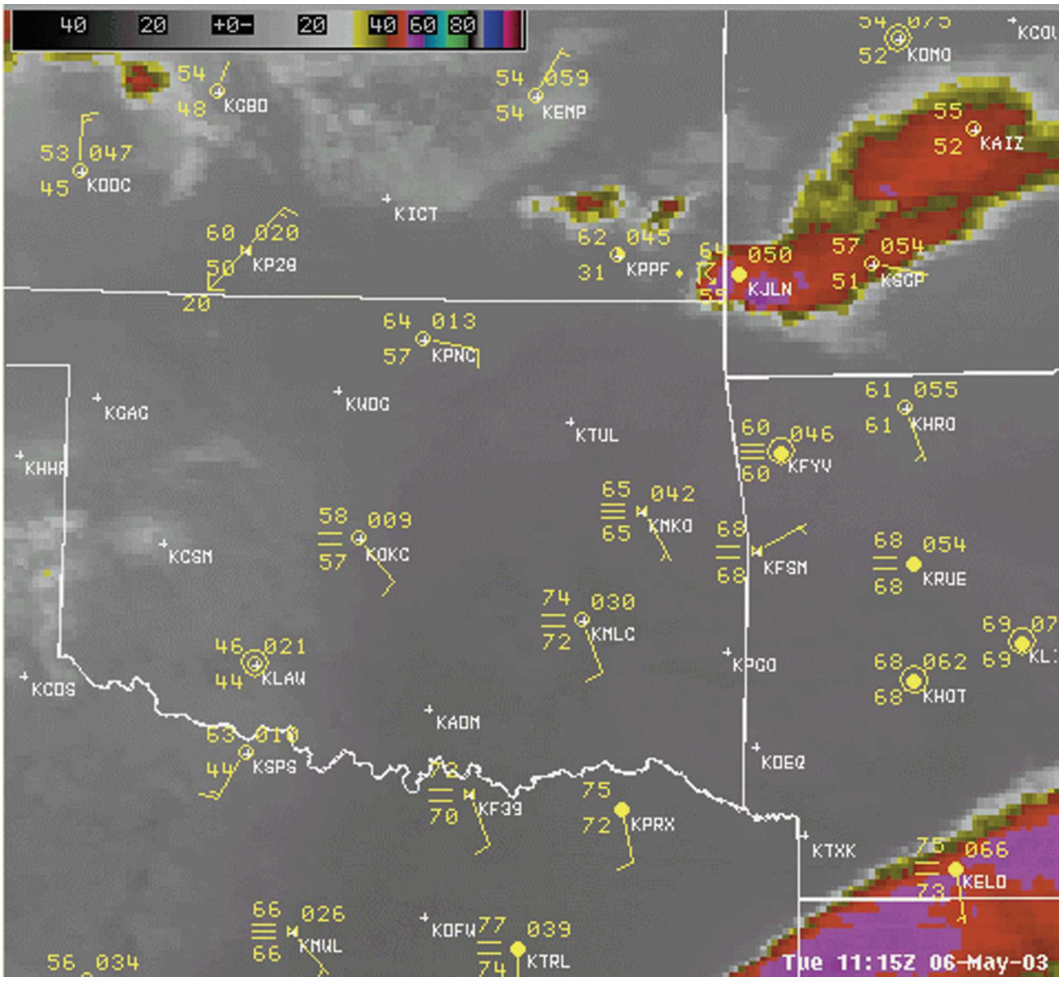

FIG. 7. *GOES-12* 10.7-μm image from 1115 UTC 6 May 2003 with surface observations overlaid. Station plots are U.S. convention. Note that the station KPFF in southeast Kansas has an instrument error for the dewpoint temperature.

Mexico was very dry and cool, and that the resulting low-level brightness temperatures were also relatively cool (brighter). Sky-cover observations (not shown) revealed that both air masses were relatively cloud free. The encroaching more unstable air was warmer and quite evident (darker) on the imagery. Here, warm, moist air is replacing a significantly cooler, drier air mass, and the difference in temperature is fairly easy to see. Recall the opposite was true in our daytime example above. Therefore, the forecaster should keep in mind the time of day to correctly identify the moist air mass, allowing nearly continuous tracking of the low-level moisture day and night. The soundings in Fig. 6 imply the advection of low-level moisture through Midland, Texas. Soundings can be used to determine the depth of the moisture to the degree that the sounding is representative of the environment. A blend of the satellite imagery and surface observations can be utilized to pinpoint the location of the moisture.

3. Examples of returning moisture in cloudy or mostly cloudy skies

In cloudy situations, infrared channels sometimes work better in combination. Dostalek et al. (1997) describe how a combination of GOES 3.9- and 10.7-μm imagery may provide a better choice as a tool to identify and track low-level boundaries at night. Briefly, the technique relies on the fact that in liquid water clouds the emissivity at 3.9 μm is lower than that at 10.7 μm. Therefore, thick low-level water clouds will appear cooler at 3.9 than at 10.7 μm. The image representing the difference between the two channels is often referred to by forecasters as the "fog product" and is

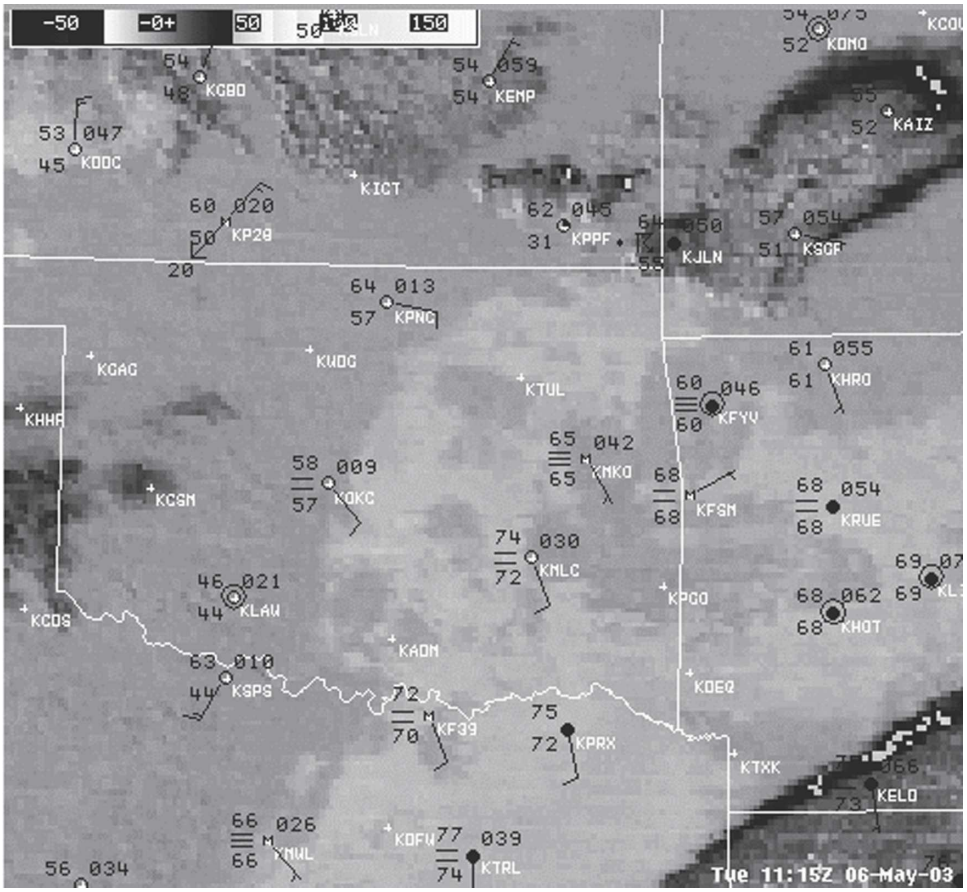

FIG. 8. *GOES-12* fog product image from 1115 UTC 6 May 2003 with surface observations overlaid. The color table highlights liquid clouds with lighter colors and ice cloud with darker colors. Station plots are U.S. convention. Note that the station KPFF in southeast Kansas has an instrument error for the dewpoint temperature.

extremely effective in identifying low-level stratus and fog. Unfortunately, this product is also sensitive to reflected solar radiation, which complicates its usage during the day. However, visible imagery fills the gap during this critical period.

a. Example 1: Fog product at night (cloudy skies)

In some cases, the cloud-top temperatures associated with low-level stratiform cloudiness are not cool enough to provide a sharp contrast with cool ground at night. In such cases, the 10.7-μm imagery alone is not effective. As mentioned above, the fog product is designed to detect low-level water clouds. To illustrate the utility of this product, we present an example of a surface warm front that moved across the state of Oklahoma into Kansas on 6 May 2003. The returning low-level moisture was expected to combine with daytime heating to produce severe thunderstorms in southeast Kansas and southern Missouri later in the day. In this case, the 10.7-μm image from 1115 UTC (Fig. 7) does not show a clear demarcation of air masses, even though, with careful study, one can see a slight darkening in the warmer air mass. The fog product at the same time, however (Fig. 8), clearly reveals the presence of stratiform cloudiness in eastern Oklahoma and Texas. Surface observations should be overlaid to confirm that the low-level clouds are associated with low-level moisture in the warm sector. The combination of surface (buoy) observations and the fog product yield a precise, and temporally frequent, location of low-level moisture over land (water). Animation of the 15-min interval fog product imagery (not shown) along with overlaid hourly surface observations, makes tracking returning low-level air masses easier and more accurate than by use of surface data alone.

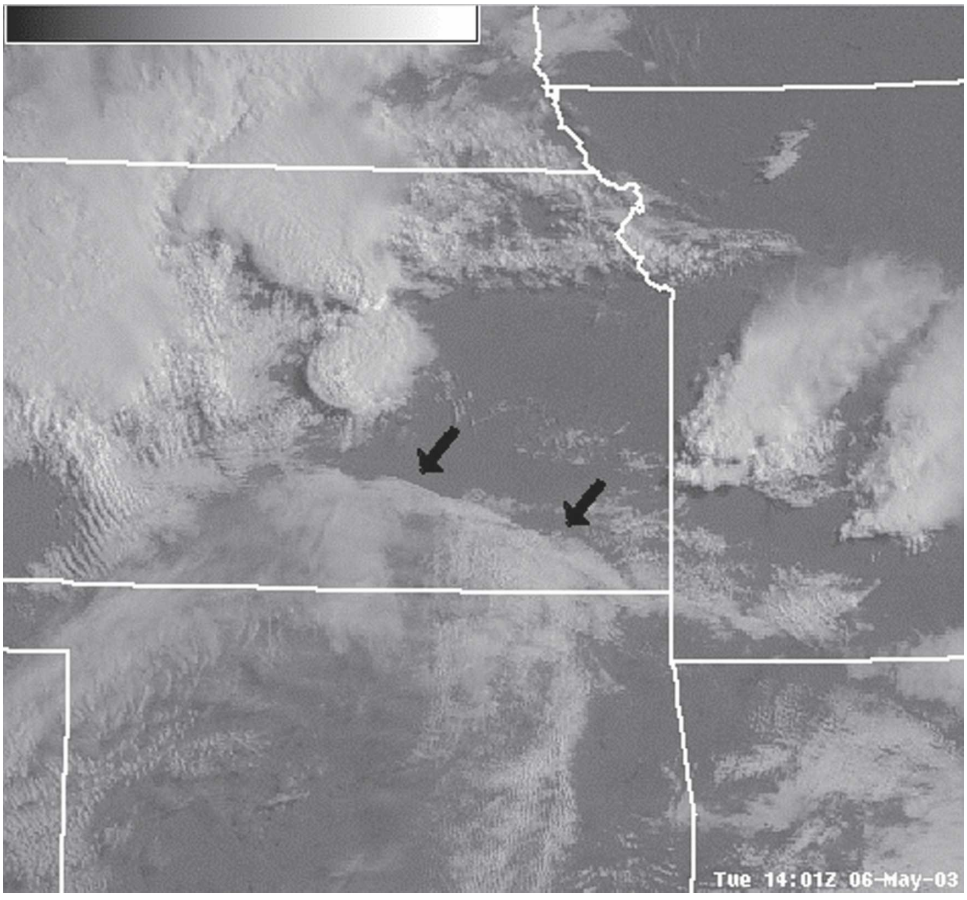

FIG. 9. *GOES-12* visible wavelength image from 1401 UTC 6 May 2003 showing the leading edge of low-level cloudiness associated with the returning low-level moisture (arrows) advecting into south-central Kansas.

b. Example 2: Visible imagery during the day (mostly cloudy skies)

Figure 9 is a visible image from later in the morning. At this time, the returning moisture had just crossed into southern Kansas and was well south of some elevated convection in central Kansas. Figure 10 shows the same convection after the warm sector air has arrived. Notice the change in appearance of the easternmost storm in Kansas from Fig. 9 to Fig. 10. During this time, the storm has intensified and now displays several features associated with severe supercell storms (Weaver and Lindsey 2004) including overshooting tops and inflow feeder clouds. It is interesting that storm intensification correlates well with the arrival of the moisture boundary. According to *Storm Data* (NCDC 2003), hail diameter sizes increased from 0.75 to 2.25 in. (19.1 mm to 57.2 mm) between 1615 and 1645 UTC.

4. Concluding remarks

Low-level moisture is an important ingredient in the development of severe weather weather situations. During the winter and spring months, low-level moisture can be cut off when cold fronts—with their attendant northerly winds, cooler temperatures, and low humidity—sweep in from the north. The forecast problem then becomes one of anticipating the northward advection of warm, moisture-laden gulf air. Understanding when to use infrared imagery, visible imagery, or the fog product and to what extent infrared satellite imagery will change diurnally, is useful in identifying the returning low-level moist air mass. The role of satellite imagery is to pinpoint the location of the low-level moist air mass (because the surface observations only give a coarse representation of location), then blend this information with the quantitative analysis of surface observations and upper-air soundings. The result of this approach is both an improved quantitative analysis and subjective analysis of low-level moisture. In the future, *GOES-R* (planned for launch in 2012) will deliver higher spatial and temporal resolution satellite imagery, further increasing the value of this technique.

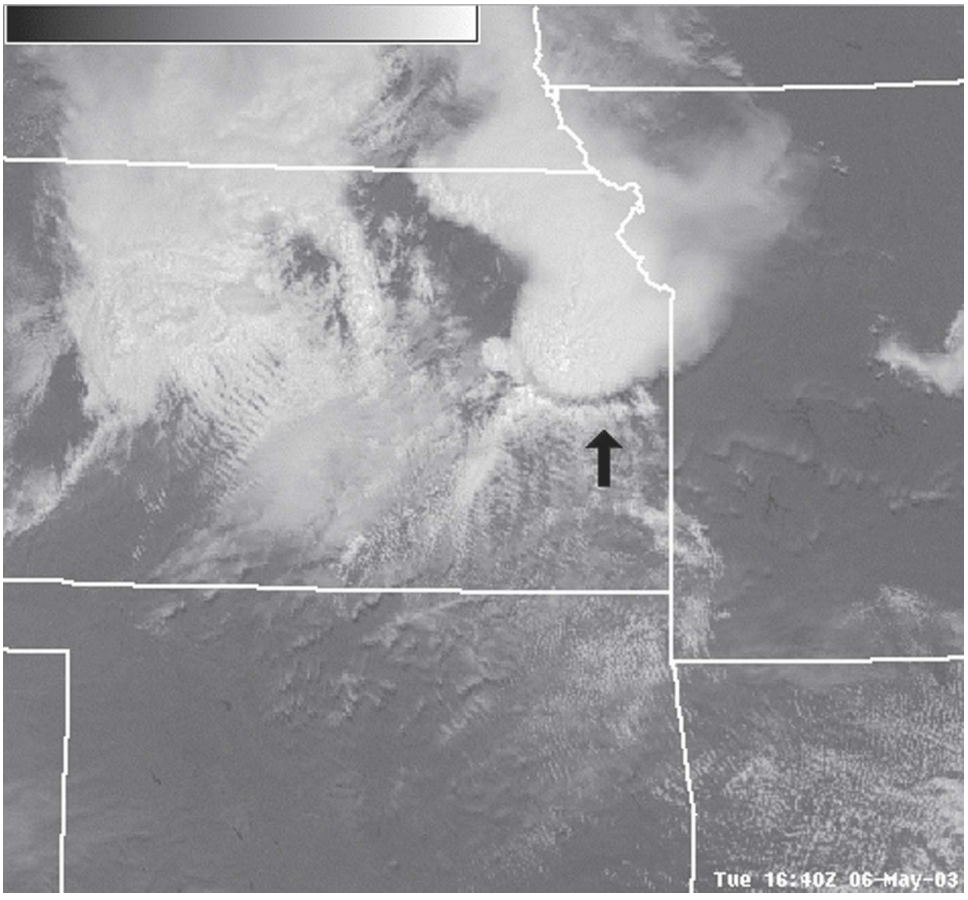

FIG. 10. *GOES-12* visible wavelength image from 1640 UTC 6 May 2003. Returning, low-level moisture has intersected the convection in central Kansas (see Fig. 9). Inflow feeder clouds indicated by arrow.

Acknowledgments. The material presented in this note was developed as part of the Virtual Institute for Satellite Integration Training (VISIT) program, which is supported under NOAA Grant NA17RJ1288. Special thanks to Timothy Schmit and Scott Lindstrom for assisting in some of the figures. Figure 6 is courtesy of the Department of Atmospheric Science, University of Wyoming. The authors express appreciation to CIRA reviewers Dr. John Knaff, Jack Dostalek, and Daniel Lindsey. Views or opinions expressed herein are those of the authors and should not be construed as an expression of official National Oceanic and Atmospheric Administration position or policy.

REFERENCES

Appleby, J. F., 1954: Trajectory method of making short-range forecasts of differential temperature advection, instability, and moisture. *Mon. Wea. Rev.,* **82,** 320–334.

Bevis, M., S. Businger, T. A. Herring, C. Rocken, R. A. Anthes, and R. H. Ware, 1992: GPS Meteorology: Remote sensing of atmospheric water vapor using the Global Positioning System. *J. Geophys. Res.,* **97,** 15 787–15 801.

Crisp, C. A., and J. M. Lewis, 1992: Return flow in the Gulf of Mexico. Part I: A classificatory approach with a global historical perspective. *J. Appl. Meteor.,* **31,** 868–881.

Dostalek, J. F., J. F. Weaver, J. F. W. Purdom, and K. Y. Winston, 1997: Nighttime detection of low-level thunderstorm outflow using a GOES multispectral image product. *Wea. Forecasting,* **12,** 947–950.

Fawbush, E. J., R. C. Miller, and L. G. Starrett, 1951: An empirical method for forecasting tornado development. *Bull. Amer. Meteor. Soc.,* **32,** 1–9.

Feltz, W. F., W. L. Smith, R. O. Knuteson, H. E. Revercomb, H. M. Woolf, and H. B. Howell, 1998: Meteorological applications of temperature and water vapor retrievals from the ground-based atmospheric emitted radiance interferometer (AERI). *J. Appl. Meteor.,* **37,** 857–875.

Henry, W. K., 1979a: Some aspects of the fate of cold fronts in the Gulf of Mexico. *Mon. Wea. Rev.,* **107,** 1078–1082.

——, 1979b: An arbitrary method of separating tropical air from "return flow" polar air. *Natl. Wea. Dig.,* **4,** 22–26.

Humphreys, W. J., 1926: The tornado. *Mon. Wea. Rev.,* **54,** 501–503.

Johnson, J. R., 1976: The origin, structure, and modification of

return flow over the Gulf of Mexico. M.S. thesis, Department of Meteorology, Texas A&M University, 69 pp. [Available from Dept. of Meteorology, Texas A&M University, College Station, TX 77843.]

Karnavas, G. R., 1978: On polar air modification over the Gulf of Mexico during periods of return flow and development of low clouds. M.S. thesis, Department of Meteorology, Texas A&M University, 69 pp. [Available from Dept. of Meteorology, Texas A&M University, College Station, TX 77843.]

Lewis, J. M., and A. C. Crisp, 1992: Return flow in the Gulf of Mexico. Part II: Variability in return-flow thermodynamics inferred from trajectories over the gulf. *J. Appl. Meteor.,* **31,** 868–881.

——, C. M. Hayden, R. T. Merrill, and J. M. Schneider, 1989: GUFMEX: A study of return flow in the Gulf of Mexico. *Bull. Amer. Meteor. Soc.,* **70,** 24–29.

Menzel, P. W., and J. F. W. Purdom, 1994: Introducing GOES-I: The first of a new generation of Geostationary Operational Environmental Satellites. *Bull. Amer. Meteor. Soc.,* **75,** 757–781.

Miller, R. C., 1972: Notes on the analysis and severe storm forecasting procedures of the Air Force Global Weather Central. AWS Tech. Rep. 200 (revised), Air Weather Service, Scott Air Base, IL, 190 pp. [Available from the National Technical Information Service, 5285 Port Royal Rd, Springfield, VA 22151.]

NCDC, 2003: *Storm Data*. Vol. 45, No. 5, 456 pp.

Newton, C. W., 1963: Dynamics of severe convective storms. *Severe Local Storms, Meteor. Monogr.*, No. 27, Amer. Meteor. Soc., 33–58.

Parmenter, F. C., 1976: Low-level moisture intrusion from infrared imagery. *Mon. Wea. Rev.,* **104,** 100–104.

Rabin, R. M., L. A. McMurdie, C. M. Hayden, and G. S. Wade, 1991: Monitoring precipitable water and surface wind over the Gulf of Mexico from microwave and VAS satellite imagery. *Wea. Forecasting,* **6,** 227–243.

——, ——, ——, and ——, 1992: Layered precipitable water from the infrared VAS sounder during a return-flow event over the Gulf of Mexico. *J. Appl. Meteor.,* **31,** 819–830.

——, ——, ——, and ——, 1993: Evaluation of the atmospheric water budget following an intense cold-air outbreak over the Gulf of Mexico—Application of a regional forecast model and SSM/I observations. *J. Appl. Meteor.,* **32,** 3–16.

Schaefer, J. T., 1986: Severe thunderstorm forecasting: A historical perspective. *Wea. Forecasting,* **1,** 164–189.

Schwartz, B. E., and C. A. Doswell III, 1991: North American rawinsonde observations: Problems, concerns, and a call to action. *Bull. Amer. Meteor. Soc.,* **72,** 1885–1896.

Showalter, A. K., and J. R. Fulks, 1943: Preliminary report on tornadoes. U.S. Dept. of Commerce, Weather Bureau, No. 806, 162 pp.

Weaver, J. F., and D. Lindsey, 2004: Some frequently overlooked severe thunderstorm characteristics observed on GOES imagery: A topic for future research. *Mon. Wea. Rev.,* **132,** 1529–1533.

Weiss, S. J., 1992: Some aspects of forecasting severe thunderstorms during cool-season return-flow episodes. *J. Appl. Meteor.,* **31,** 964–982.

Whitney, L. F., Jr., and J. E. Miller, 1956: Destabilization by differential advection in the tornado situation 8 June 1953. *Bull. Amer. Meteor. Soc.,* **37,** 224–229.